Protocol to define material behaviour and failure strain level at low and high strain rates based on compression test

Tomasz Jankowiak, Alexis Rusinek, Amine Bendarma

JOURNAL OF THEORETICAL AND APPLIED MECHANICS
56, 2, pp. 471-481, Warsaw 2018
DOI: 10.15632/jtam-pl.56.2.471

PROTOCOL TO DEFINE MATERIAL BEHAVIOUR AND FAILURE STRAIN LEVEL AT LOW AND HIGH STRAIN RATES BASED ON A COMPRESSION TEST

Tomasz Jankowiak
Poznan University of Technology, Institute of Structural Engineering, Poznań, Poland
e-mail: tomasz.jankowiak@put.poznan.pl

Alexis Rusinek
Laboratory of Microstructure Studies and Mechanics of Materials, UMR-CNRS 7239, Lorraine University, Metz Cedex, France

Amine Bendarma
Poznan University of Technology, Institute of Structural Engineering, Poznań, Poland, and Universiapolis, Ecole Polytechnique d'Agadir Bab Al Madina, Agadir, Morocco

Compression test is frequently used to define material behaviour. However, this test may be depending on different effects, for example friction, specimen inertia or local stress triaxiality. For this reason, a new design is proposed to analyse the previous effects and to try to minimize it on quantities measured as macroscopic stress and strain. To have a complete understanding, numerical simulations have been performed using finite element method (Abaqus/Standard and Abaqus/Explicit). It allows one to define the macroscopic behaviour and to have an access to the local values not accessible during experiments for a better understanding of the experimental measurements.

Keywords: stress triaxiality, dynamic compression, material behaviour, numerical simulation

1. Introduction

The shape and dimensions of the specimen used during experiments have an important effect on experimental measurements in both static and dynamic loadings. In general, to define the behaviour of a material $\sigma(\varepsilon, \dot{\varepsilon}, T)$, different tests are frequently used: compression, tension, shear, biaxial compression. In this paper, static and dynamic compression tests are considered. This kind of experiments is used to define the behaviour of materials at low and high strain rates and to verify the symmetry of the yield surface comparing to tension, but it induces some problems as it will be discussed in details in this paper. One of the main problems is related to the friction effect between the specimen and the plateau or the split Hopkinson pressure bars (SHPB). This phenomenon is related to the quality of contact and state (lubricated or dry) and it is defined using the friction coefficient value μ. This effect is crucial since it may induce an overstress state as discussed in details in (Jankowiak *et al.*, 2011). Some other quantities are also disturbing the measurements under dynamic loading and using SHPB. These are local inertia of the specimen, puncture of the bars (Safa and Gary, 2010; Małachowski *et al.*, 2014), elastic wave dispersion and shape of the contact zone projectile end – input bar. As observed in (Jankowiak *et al.*, 2011), the stress state is changing when the friction coefficient increases on the contact side. Therefore, an uniaxial compression state cannot be assumed. In the dynamical state, as it was discussed in some papers (Jankowiak *et al.*, 2011; Iwamoto and Yokoyama, 2012; Kii *et al.*, 2014), the ratio length L – diameter D must be in a certain range of values to avoid some problems described

previously. This ratio is defined using the parameter $s = L/D$. In this work, several values of s have been used, see Fig. 1.

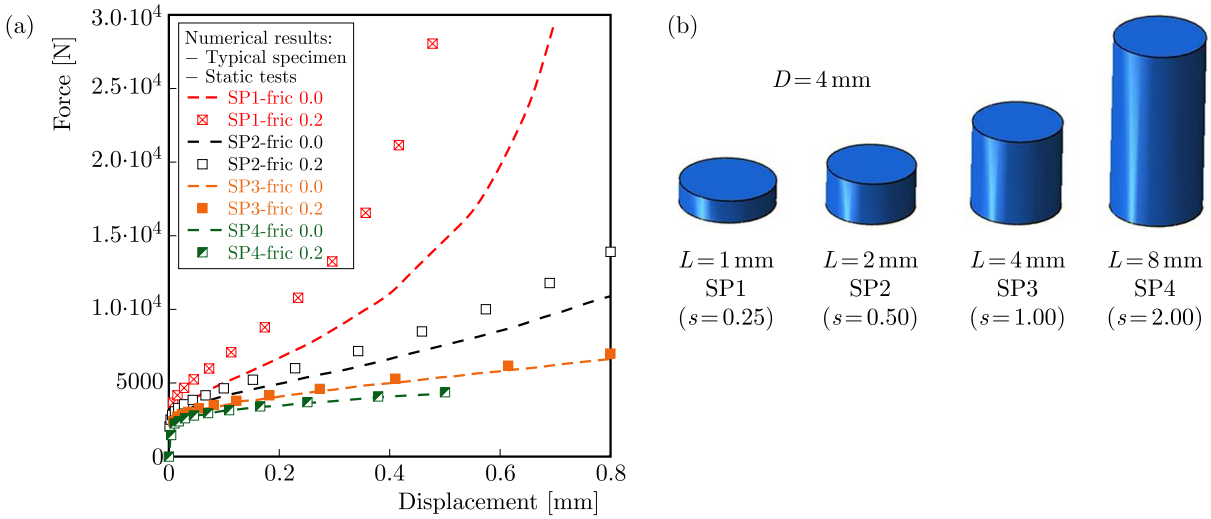

Fig. 1. Force versus displacement for quasi-static compression using standard specimen SPi

Deformation of the specimen in compression depends on the friction process, Fig. 1. The results reported in this paper are for a constant diameter $D = 4$ mm and different initial length L to vary the ratio s. Therefore, the following configurations have been used: SP1 ($s = 0.25$) with a length of 1 mm and SP4 ($s = 2.0$) with a length of 8 mm. The intermediate specimens SP2 and SP3 have, respectively, a length of 2 mm and 4 mm. It corresponds to a value of s equal to 0.5 and 1.0. The results (force versus displacement curve) for a friction coefficient varying from 0.0 to 0.2 are presented in Fig. 1. In general and following some recommendations, the ratio s equal to 0.5 is frequently used during dynamic tests to avoid some of the problems discussed previously. However, for this ratio, the friction effect is visible (comparing the curves SP2-fric 0.0 and SP2-fric 0.2), see Fig. 1. In the previous picture, Fig. 1, it is observed that the friction coefficient is acting strongly on the specimen having the shortest active length (SP1). In this paper, modified specimens SPiM, Fig. 2, are used to measure during experiments the intrinsic material behaviour. The SPiM results will be compared to the original ones to observe if the friction effect may be reduced using a new design. To confirm it, some comparisons will be reported in terms of the force-displacement curve changing the friction coefficient μ. The same ratio s has been considered between SPi and SPiM.

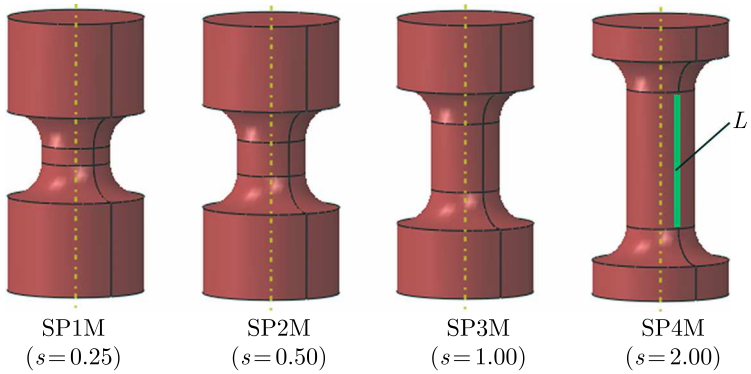

Fig. 2. Modified specimen design SPiM for the compression test under quasi-static and dynamic compression

2. Geometric effect on the compression force measurement using SP*i*M specimen

The variation of the stress state defined by η has an effect on the measured force and, in the same way, on the final macroscopic stress level σ estimated during experiments and simulations. Another important parameter is related to the specimen shape ratio s which is inducing a change of the stress triaxiality η, as it will be discussed in this paper. This variable is related to the ratio of the hydrostatic stress p and to the Huber-Mises equivalent stress q. To reduce this phenomenon, a new geometry design is proposed, Fig. 2. The specimens are named SP*i*M with $i = 1$ to 4 corresponding, respectively, to an active part of 1 mm, 2 mm, 4 mm and 8 mm. Based on it, the shape ratio s is calculated. It corresponds to the ratio of the initial length L divided by the diameter of the active part of the specimen D. For the new geometry, the ratio is respectively equal to 0.25, 0.5, 1.0 and 2.0. To analyze the geometric effect, the following constitutive relation, Eq. (2.1), has been used in FE code. Therefore, just hardening has been considered. The strain rate sensitivity as the temperature sensitivity is not taking into account

$$\sigma = A + B\varepsilon_P^n \tag{2.1}$$

Two material behaviours are assumed, see Table 1, allowing one to demonstrate that the results are just related to geometry and not to material behaviour. Thus, this analysis and geometry can be used with all materials assumed or studied.

Table 1. Constants used to define mild steel ES and aluminum AA6060 assuming Eq. (2.1)

	Mild steel ES (Jankowiak *et al.*, 2011)	Aluminium AA6060 (Beusink, 2011)
Young modulus E	200 GPa	70 GPa
Yield stress A	154 MPa	70 MPa
Strain hardening B	464 MPa	302 MPa
Strain hardening n	0.37	0.46

The behaviour is depicted in Fig. 3 for a larger yield stress and hardening of mild steel.

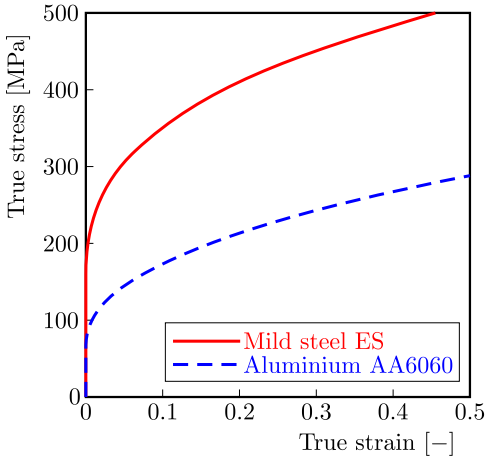

Fig. 3. Comparison of true stress – true strain curve for two different materials

To analyse how the geometry may act on the material behaviour definition using different geometries, mild steel has been considered in the first part of numerical simulations, see Table 1 and Fig. 3. The results for all geometries and two values of the friction coefficient μ are reported in Fig. 4.

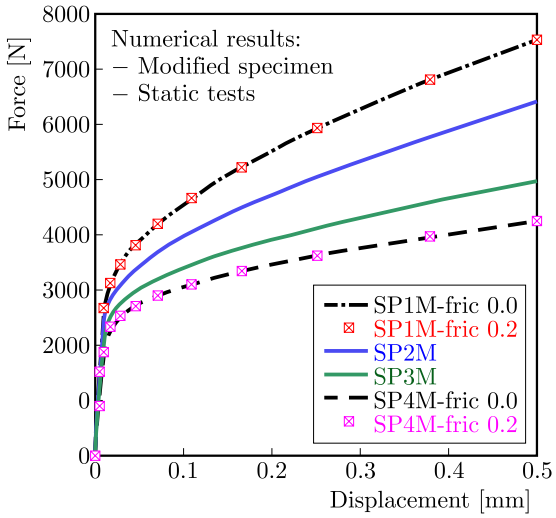

Fig. 4. Force versus displacement for quasi-static compression using the modified specimen SPiM for mild steel

Using the same material behaviour and the same diameter D, it is observed that the material behaviour is depending on the active length of the specimen. On the contrary, the friction coefficient is not acting as it was observed in (Jankowiak *et al.*, 2011). Based on the previous results, it is observed that the ratio s is responsible for different behaviours in terms of force--displacement relationship. To analyse the local distribution of the stress triaxiality with plastic deformation, numerical simulations have been used. Thus, it is observed that the stress triaxiality is equal to -0.34 for $s = 2.0$ (SP4M) which corresponds to the compression value equal to $-1/3$, Fig. 5. The results are reported for each geometry in the following picture, Fig. 5.

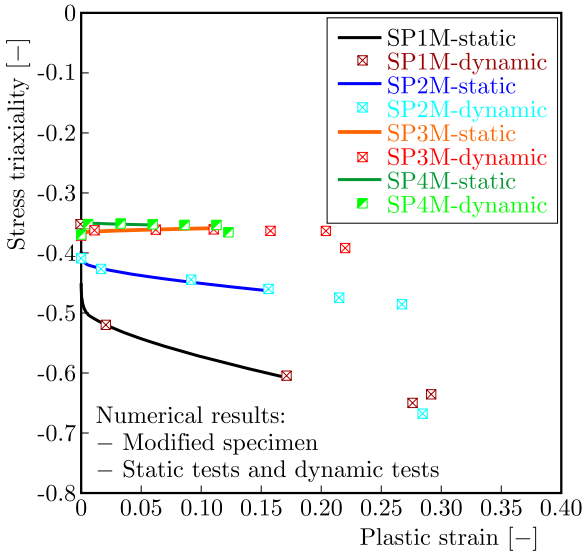

Fig. 5. Average stress triaxiality versus plastic strain for all modified specimens SPiM (static and dynamic loadings using numerical simulations)

It can be seen that η is varying from -0.58 to -0.65 for SP1M and from -0.42 to -0.47 for SP2M. For SP3M, the value is not depending on the plastic strain level and is equal to -0.36. To estimate the local inertia due to the mass added to both sides of the standard specimen, Fig. 2, numerical simulations have been done at a high velocity $V_0 = 10\,\mathrm{m/s}$. As the strain rate sensitivity of the material is not considered, Eq. (2.1), the difference in terms of the force

may be due to the mass inertia only. Based on numerical simulations, it is observed that the masses added do not affect the results and, in the same way, do not affect the macroscopic stress (triaxiality) and strain level, Fig. 5. In the following part of the text, the case corresponding to high velocity coupled with the inertial effect is defined as dynamic, and the second case corresponding to low velocity is named static.

In the following curves, Fig. 6, two cases are reported considering the geometry SP1 and SP4 (standard specimens) for different friction coefficients. It is observed for the shortest specimen SP1 that the friction coefficient induces a strong increase of the stress triaxiality η. In the range of plastic deformation considered, the value is varying from 0.6 to 1.5. For SP4, the stress triaxiliaty is more stable and the value is close to the compression state with $\eta = -1/3$.

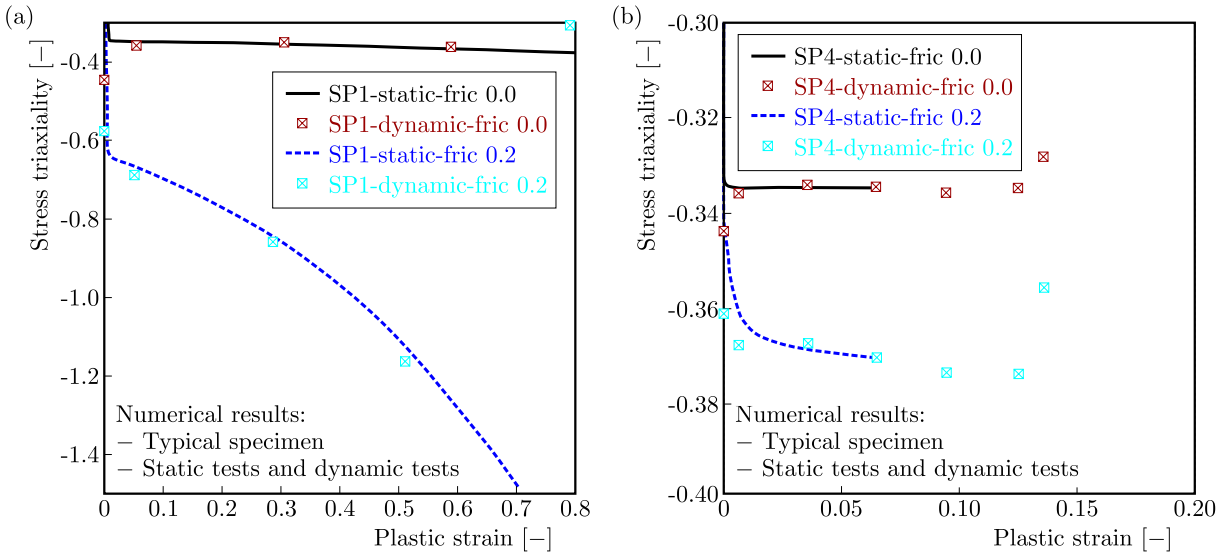

Fig. 6. Average stress triaxiality for standard specimens (SP1 and SP4) for friction coefficients 0.0 and 0.2

3. Material behaviour definition and analysis

For the standard shape specimen SPi, the behaviour of the material in static and in dynamic conditions can be obtained using the friction correction as discussed in details in (Jankowiak *et al.*, 2011; Zhong *et al.*, 2015). The friction coefficients μ changes the process of plastic deformation and the stress state. Finally, the compressive test with friction coefficient $\mu > 0$ does not predict uniaxial behaviour, and the stress triaxiality η decreases to $-1/3$. Using the modified geometry design SPiM, friction correction is not required. However, the state of the stress does not correspond to uniaxial compression.

For SPi geometry and in order to correct the friction coefficient effect, the model proposed by Klepaczko-Malinowski may be used as described in (Jankowiak *et al.*, 2011; Klepaczko and Malinowski, 1977). In a simplified approach and considering that the inertia and the second derivative of the strain rate effect may be neglected, the correction is the following, Eq. (3.1). Therefore, just the geometry effect is taken into account

$$\sigma_{mat} = \sigma_{meas}\left(1 - \frac{\mu}{3s}\right) = \sigma_{meas} C \tag{3.1}$$

where σ_{mat} is the stress in the material and σ_{meas} is the stress measured in the compression test. Using numerical results, the geometrical variable C may be defined for all cases considered SPi. The value vary from 0.733 to 0.967 considering, respectively, SP1 to SP4, Table 2. In this analysis the friction coefficient is assumed to be equal to 0.2.

Table 2. Definition of the variable C for all cases considered SPi, Eq. (3.1)

	s	C
SP1	0.25	0.733
SP2	0.5	0.867
SP3	1	0.933
SP4	2	0.967

The method of correction is working correctly for a material without or with reduced plastic strain hardening like pure copper in (Jankowiak *et al.*, 2011). The numerical results (stress-strain curve) are presented for SP4 (the longest) and SP1 (the shortest) in Fig. 7. For a material with strain hardening, the gap between the input model and the method proposed by Klepaczko-Malinowski does not allow one to correctly define the intrinsic behaviour of the material for strain levels $\varepsilon > 15$. For larger plastic deformation levels, the stress state is more complex due to the friction effect and the previous method based on the friction correction is not enough. However, it is observed that the friction effect may be neglected for specimen SP4, see Figs. 7 and 8b.

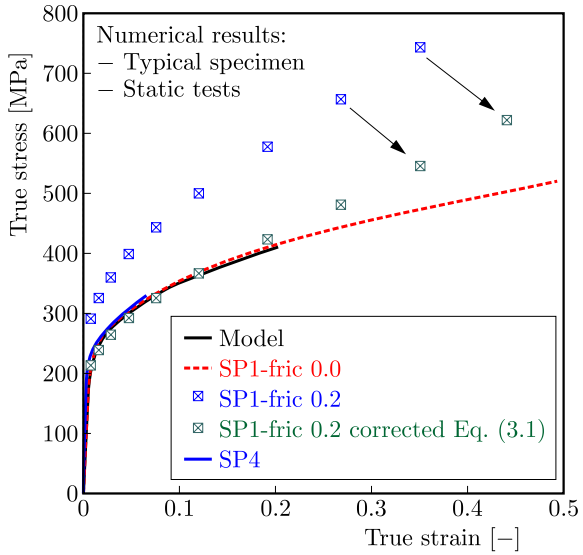

Fig. 7. True stress – true strain curve for the standard specimen

If the specimen length decreases the stress state is changing as reported, Fig. 6. For the specimen SP1, and assuming that the friction coefficient is equal to zero, the numerical results in terms of behaviour are in agreement with the constitutive relation used as an input, Fig. 7. If the friction coefficient increases, $\mu > 0$, a correction is necessary (Jankowiak *et al.*, 2011). Using numerical calculations, two quantities are defined, the Huber-Mises σ_{Mises} equivalent stress and the longitudinal stress σ_{yy} corresponding to the axial loading direction. It has to be noticed that during experiments, the longitudinal stress is the one corresponding to the stress imposed to the specimen. The value of σ_{yy} is obtained dividing the force by the cross section of the specimen. Using these two quantities, the parameter α may be defined. It consists in dividing the longitudinal stress by the equivalent stress as $\alpha = \sigma_{yy}/\sigma_{Mises}$. The value is equal to 1 for uniaxial compression. In other cases, α is varying with the level of plastic deformation as observed for the stress triaxiality, Fig. 8a. To demonstrate this effect, the results for SP4 (the longest) and SP1 (the shortest) are presented in Fig. 8b. If the stress measured during experiments is divided by the α parameter, the material behaviour obtained from numerical simulations is in

agreement with the constitutive relation used. This method is working correctly also for material with plastic strain hardening.

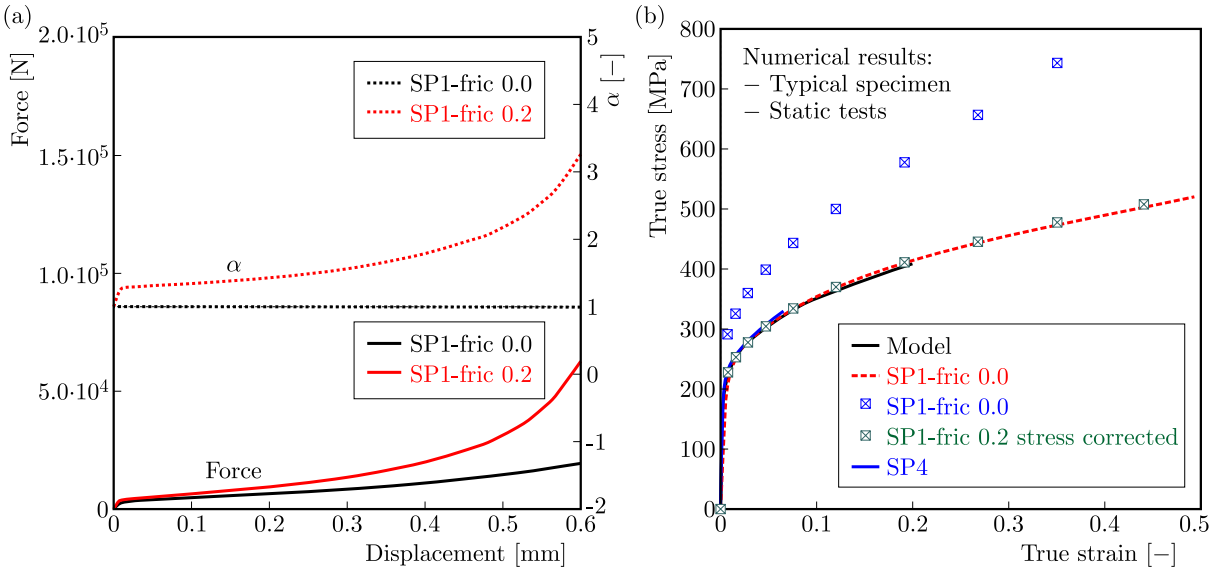

Fig. 8. (a) Influence of the friction coefficient on the measured force and α for model SP1; (b) true stress – true strain curve for the standard specimen SPi with stress correction for mild steel ES

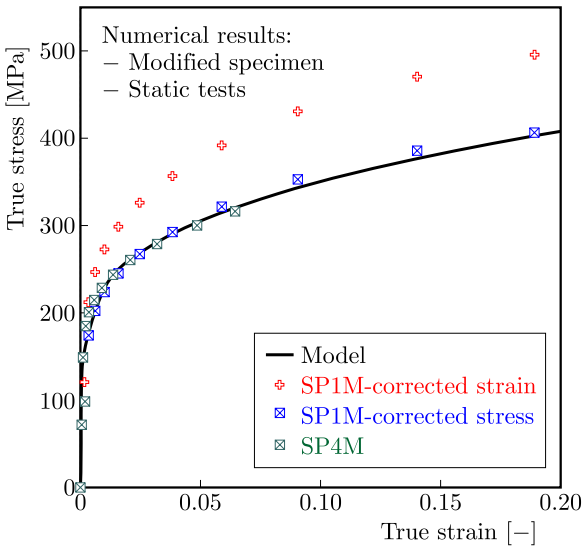

Fig. 9. True stress versus true strain curve for modified specimens under quasi-static loading using mild steel

The specimen modified SPiM has been used to eliminate the friction effect on the stress-strain curve. As demonstrated before, the friction effect was not observed using SPiM, Fig. 4. The true stress-true strain curve for SP4M with and without friction give the same results in agreement with the constitutive relation used, Eq. (2.1), see Fig. 9. However, the triaxiality influence the measured stress as observed for the standard specimen. Analysing the current results, it is visible that these new modified specimens SPiM are much better in describing the failure strain and failure criterion of the materials. However, using these modified short specimens to predict material behaviour, the difficulty is to define the equivalent effective length L_{eff}, different to that reported in Fig. 2 and Fig. 10. To estimate it, numerical simulations have been carried out. The proposed method is presented in this part for the shortest modified specimen SP1M. The

final results are reported in Fig. 9 for specimen SP1M. In this specific case, the final average strain in the active part of the specimen is equal to 0.19. However, if the final strain is calculated from displacements based on the active length of the neck part (1 mm), the final strain level will be equal to 0.551. However, using $L_{eff} = 2.86\,\text{mm}$, corresponding to the ratio of the strain level described previously, the final strain is equal to 0.19 as the average value in the active part of the specimen. This procedure allows one to correct the strain during the compression test using the modified specimen.

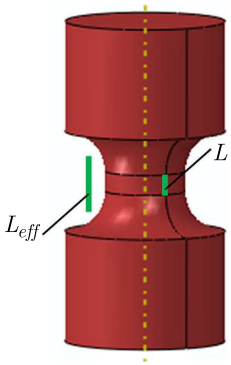

Fig. 10. Definition of the length and effective length used to calulate the strain level

The second step is to correct the stress level using the correction factor $\alpha = \sigma_{yy}/\sigma_{Mises}$. The triaxiality is not strongly changing for this kind of specimen and it is the same for α. In this case, the average value of α during compression is 1.22. To correct the stress measured during experiments or computed by FE code (Małachowski *et al.*, 2014; Dunand and Mohr, 2010), it is necessary to divide the macroscopic stress measured or calculated by 1.22 to estimate the intrinsic material behaviour. The same procedure should be done for other cases. The correction factors for stress should be every time calculated using an inverse method coupling experiments with numerical simulations. To demonstrate that the correction is directly related to the geometry and not to the material tested, numerical simulations have been performed for two materials. It is observed that the correction is related to the applied geometry and not to the material, Fig. 11. The conclusion is the same for SP1M and SP4M. Moreover, it is observed, Fig. 11, that the friction effect does not change the stress triaxiality using SP4M and is not dependent on the

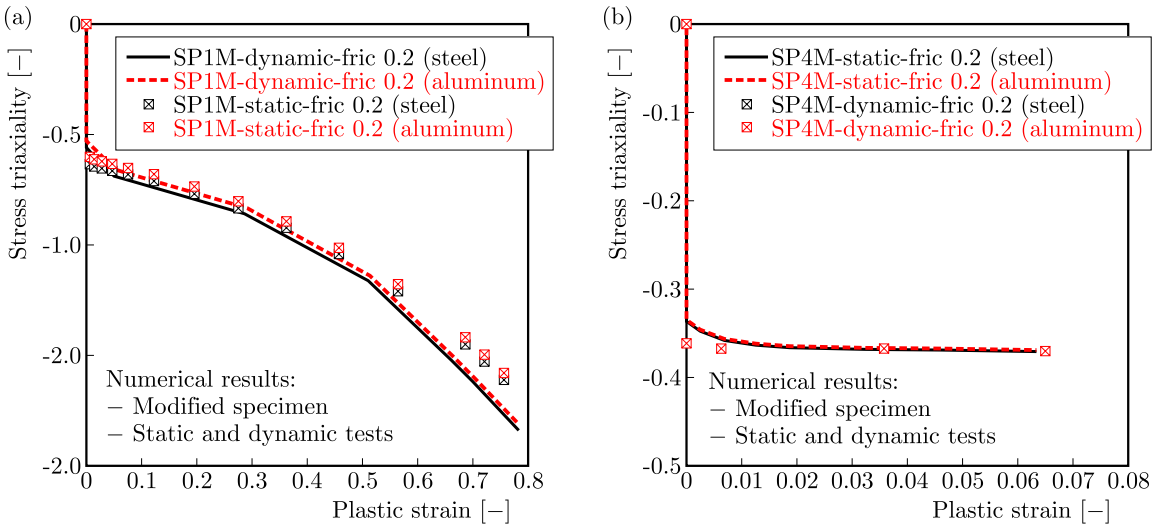

Fig. 11. Comparison of compression results (stress triaxiality versus plastic strain); (a) SP1M and (b) SP4M

material used. Therefore, SP4M may be used to define the material behaviour with the stress triaxiality state corresponding to compression.

Finally, the strain and stress are corrected using Eqs. $(3.2)_4$ and $(3.2)_2$, respectively.

$$\varepsilon_{mat} = \kappa_{SPiM}\varepsilon_{meas} \qquad \sigma_{mat} = \lambda_{SPiM}\sigma_{meas} \tag{3.2}$$

where λ_{SPiM} and κ_{SPiM} are the geometric coefficients allowing one to define the intrinsic behaviour of the material $\sigma(\varepsilon)$. The first coefficient is related to $1/\alpha$ and the second one to L/L_{eff}. Depending on the geometry SPiM, to obtain the material behaviour, the following corrections are necessary, Table 3.

Table 3. Geometric coefficients for material behaviour definition using SPiM coupled to Eqs. (3.2)

Geometry design, length	λ_{SPiM}	κ_{SPiM}	L_{eff}
SP1M $L = 1$ mm	0.82	0.35	2.86
SP2M $L = 2$ mm	0.92	0.58	3.45
SP3M $L = 4$ mm	0.98	0.78	5.13
SP4M $L = 8$ mm	1	1	8

In addition to material behaviour characterization and for some materials with a reduced ductility, the failure strain ε_f level may be estimated depending on the stress triaxiality, Eq. (3.3). The presented results demonstrate that the use of the specimens with modified shape SPiM in compression tests gives promising results and allows one to eliminate the friction effect, which increases the measured stress as observed during experiments

$$\varepsilon_f = f(\eta) \tag{3.3}$$

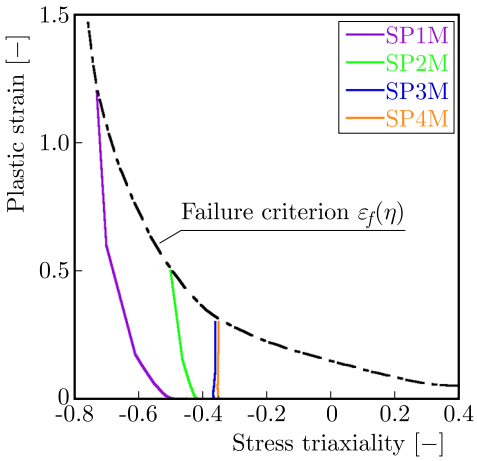

Fig. 12. Failure criterion definition – failure plastic strain as a function of the stress triaxiality η

This kind of approach was previously proposed in shear by Rittel *et al.* (2002). The specimen was used to estimate, after some corrections, the material behaviour and the failure strain level as well. The values of the failure strain level for the new specimens SPiM are reported Fig. 12. The value of triaxiality η is varying from -0.7 to -0.36. A general example is shown in Fig. 12 and demonstrates how the stress triaxiality changes with plastic deformation mainly for SP1M and SP2M. Using SP3M or SP4M, the value is relatively constant and close to the compression state. An other advantage of having different values of η is the ability precisely define constants of some failure criteria (Bao and Wierzbicki, 2004; Wierzbicki *et al.*, 2005; Rusinek *et al.*, 2007; Dunand and Mohr, 2011), see for example the Johnson-Cook model, Fig. 12.

Now, coupling the new design SP*i*M with the specimen proposed by Rittel *et al.* (2002), the failure strain level ε_f may be defined for the stress triaxiality η varying between $-0.66 \leqslant \eta \leqslant -0.33$ depending on the shear angle inclination. It is also possible to perform, in an easy way, a tensile test to reach a value of $\eta = 0.33$.

4. Conclusions

From the numerical results, it can be seen that using the new design of the compression specimen does not allow one to define the material behaviour without the friction effect only, but also enables estimation of the failure strain level depending on the stress triaxiality. The tests may be complementary to other tests such as tension, shear or biaxial compression (Frąś *et al.*, 2014; Field *et al.*, 2001; Davies and Hunter, 1963; Baranowski *et al.*, 2014).

Thus, comparing all results and basing on the systematic analysis, it is clear that the best solution in terms of the material behaviour is to use the geometry modified SP4M, Fig. 2.

Moreover, it is demonstrated that the parameters calculated to estimate the material behaviour are not dependent on the material used but only on the geometry of SP*i*M.

References

1. Bao Y., Wierzbicki T., 2004, On fracture locus in the equivalent strain and stress triaxiality space, *International Journal of Mechanical Sciences*, **46**, 81-98
2. Baranowski P., Janiszewski J., Małachowski J., 2014, Study on computational methods applied to modelling of pulse shaper in split-Hopkinson bar, *Archives of Mechanics*, **66**, 6, 429-452
3. Beusink M., 2011, Measurements and simulations on the (dynamic) properties of aluminium alloy AA6060, raport of: Faculty of Mechanical Engineering, Eindhoven University of Technology, SIMLab, Department of Structural Engineering, Norwegian University of Science and Technology, Eindhoven
4. Davies E.D.H., Hunter S.C., 1963, The dynamic compression testing of solids by the method of the split Hopkinson pressure bar, *Journal of the Mechanics and Physics of Solids*, **11**, 155-179
5. Dunand M., Mohr D., 2010, Hybrid experimental-numerical analysis of basic ductile fracture experiments for sheet metals, *International Journal of Solids and Structures*, **47**, 9, 1130-1143
6. Dunand M., Mohr D., 2011, On the predictive capabilities of the shear modified Gurson and the modified Mohr-Coulomb fracture models over a wide range of stress triaxialities and Lode angles, *Journal of the Mechanics and Physics of Solids*, **59**, 7, 1374-1394
7. Field J.E., Proud W.G., Walley S.M., Goldrein H.T., 2001, Review of experimental techniques for high rate deformation and shock studies, [In:] *New Experimental Methods in Material Dynamics and Impact*, W.K. Nowacki, J.R. Klepaczko (Edit.), Vol. 3: *Trends in Mechanics of Materials*, 109-177
8. Frąś T., Rusinek A., Pęcherski R.B., Bernier R., Jankowiak T., 2014, Analysis of friction influence on material deformation under biaxial compression state, *Tribology International*, **80**, 14-24
9. Iwamoto T., Yokoyama T., 2012, Effects of radial inertia and end friction in specimen geometry in split Hopkinson pressure bar tests: A computational study, *Mechanics of Materials*, **51**, 97-109
10. Jankowiak T., Rusinek A., Łodygowski T., 2011, Validation of the Klepaczko-Malinowski model for friction correction and recommendations on Split Hopkinson Pressure Bar, *Finite Elements in Analysis and Design*, **47**, 1191-1208

11. Kii N., Iwamoto T., Rusinek A., Jankowiak T., 2014, A study on reduction of friction in impact compressive test based on the Split Hopkinson Pressure Bar method by using a hollow specimen, *Applied Mechanics and Materials*, **566**, 548-553

12. Klepaczko J.R., Malinowski J.Z., 1977, Dynamic frictional effects as measured from the Split Hopkinson Pressure Bar, [In:] *High Velocity Deformation of Solids, IUTAM Symposium*, Tokyo, Japan, Springer-Verlag, Berlin, 403-416

13. Małachowski J., Baranowski P., Gieleta R., Damaziak K., 2014, Split Hopkinson Pressure Bar impulse experimental measurement with numerical validation, *Metrology and Measurement Systems*, **21**, 1, 47-58

14. Moćko W., Kowalewski Z.L., 2011, Dynamic compression tests – current achievements and future development, *Engineering Transactions*, **59**, 3, 235-248

15. Rittel D., Ravichandran G., Lee S., 2002, Large strain constitutive behavior of OFHC copper over a wide range of strain rates using the shear compression specimen, *Mechanics of Materials*, **34**, 627-642

16. Rusinek A., Zaera R., Klepaczko J.R., 2007, Constitutive relations in 3-D for a wide range of strain rates and temperatures – application to mild steels, *International Journal of Solids and Structures*, **44**, 17, 5611-5634

17. Safa K., Gary G., 2010, Displacement correction for punching at a dynamically loaded bar end, *International Journal of Impact Engineering*, **37**, 371-384

18. Wierzbicki T., Bao Y., Lee Y.-W., Bai Y., 2005, Calibration and evaluation of seven fracture models, *International Journal of Mechanical Sciences*, **47**, 4/5, 719-743

19. Zhong W.Z., Rusinek A., Jankowiak T., Abed F., Bernier R., Sutter G., 2015, Influence of interfacial friction and specimen configuration in Split Hopkinson Pressure Bar system, *Tribology International*, **90**, 1-14

Manuscript received December 30, 2017; accepted for print February 8, 2018